Available online at www.sciencedirect.com
SCIENCE DIRECT®
Journal of Photochemistry and Photobiology A: Chemistry 164 (2004) 33–39
Journal of Photochemistry and Photobiology A:Chemistry
www.elsevier.com/locate/jphotochem

Dye-sensitized solar cells: improvement of spectral response by tandem structure

Wataru Kubo, Ayumi Sakamoto, Takayuki Kitamura, Yuji Wada, Shozo Yanagida*

Material and Life Science, Graduate School of Engineering, Osaka University, Suita, Osaka 565-0871, Japan

Received 10 September 2003; received in revised form 24 December 2003; accepted 4 January 2004

Abstract

A tandem structure was introduced to improve the spectral response of dye-sensitized solar cells (DSC) without loosing their high external quantum yield. Light absorption models of DSC were proposed, and light harvesting efficiency (LHE) and incident photon-to-current conversion efficiency (IPCE) were calculated using absorption spectra of dye-adsorbed TiO_2 electrode, electrolyte, and conducting glass support. The IPCE of single DSCs fabricated using two typical ruthenium complexes were measured to present the improvement of the spectral response without loosing their high external quantum yield by tandem structure. As a result, the tandem structured cell exhibited higher photocurrent and conversion efficiency than each single DSC mainly caused from its extended spectral response.

Keywords: Tandem; Dye-sensitized solar cell

1. Introduction

Dye-sensitized solar cells (DSC) were widely investigated since its low production cost and potentially high conversion efficiency [1]. A few ruthenium complexes with two bipyridyl ligands called as N3 [2] or N719 [3] injected electrons to the conduction band of the TiO_2 electrode with high quantum yield about one, and the solar cells showed high photoenergy conversion efficiencies up to 10%. Many attempts were made to improve the efficiency toward the practical use of this device. There are two major ways to improve the efficiency, one is the improvement of photovoltage and the other is the improvement of photocurrent of the solar cells. To improve the photovoltage, some metal oxides having more negative conduction band potential than TiO_2 such as NbO_5 [4] or $SrTiO_3$ [5] were used as a TiO_2 substitute. To improve the photocurrent, the improvement of absorbance in the longer wavelength region is important because the solar spectrum has large photon flux in a wavelength region 500–1000 nm [6] N3 or N719 dyes can absorb solar light up to 800 nm, but the absorption coefficients of these dyes at the longer wavelength region (> 600 nm) were not enough to catch photons efficiently. An approach to this issue is employing light scattering structures such as some metal oxide particles with several hundreds nanometer diameter [7,8] or a photonic crystal [9] to enhance the light path length. Employing these scattering structures succeeded to enhance photocurrent by increasing light absorption at longer wavelength region ($600 < \lambda < 800$ nm) but cannot extend the spectral response to the wavelength longer than the absorption edge of the dye. The development of sensitizing dyes to extend the absorption edge has been one of the most significant issue in this field. Several ruthenium complexes having terpyridine as a ligand called “black dye” showed extended absorption edge up to 1000 nm and converted photons to electrons [10,11]. Unfortunately sensitizers having near IR absorption tend to have lower excited-state excess free energies to the electron injection and the absorption coefficients, resulting in lower incident photon-to-current conversion efficiency (IPCE) at shorter wavelength region. These results limit their usefulness, and outstanding improvement in the conversion efficiency has not been reported yet.

Tandem structure is used in some pn junction type solar cells to improve the spectral response of the solar cells [12]. The absorption wavelength of this type of solar cell is determined by the band gaps of semiconductors used in the cells. In the case of DSC, the absorption wavelength was inherent in sensitizing dyes adsorbed on the semiconductor surface. Hence, the combination of DSCs with several dyes having different absorption wavelength should improve the total spectral response of DSC.

In this paper, we fabricated tandem DSCs using N719 and black dye. The dye, N719 exhibits high IPCE and relatively

* Corresponding author. Tel.: +81-6-6879-7924; fax: +81-6-6879-7875.
E-mail address: yanagida@mls.eng.osaka-u.ac.jp (S. Yanagida).

1010-6030/$ – see front matter © 2004 Elsevier B.V. All rights reserved.
doi:10.1016/j.jphotochem.2004.01.024

narrow spectral response, and black dye has relatively wide spectral response but is difficult to obtain high IPCE. We report that the improvement in the spectral response of DSC without loosing high IPCE at the lower wavelength region by introduction of the tandem structure using N719 and black dye.

2. Light absorption models for DSC

Light absorption models for DSC were considered to evaluate the change of photocurrent by the introduction of the tandem structure. Light harvesting efficiency (LHE) and IPCE were calculated using these models.

A photoelectrode of DSC consists of dye adsorbed nanocrystalline metal oxide particles. It is difficult to evaluate the light absorption by sensitizing dyes accurately since an electrolyte penetrates into the porous electrode. A light absorption model that the cell consists of the stacks of the dye-adsorbed TiO_2 film layer and the electrolyte layer having infinitesimal thickness was proposed. With this assumption, the LHE and the IPCE [2] of a single DSC are described as:

$$\mathrm{LHE_{S(D)}} = T_{\mathrm{FTO}}\left(1 - 10^{-(A_{\mathrm{D}}+A_{\mathrm{E}}P)}\right)\frac{A_{\mathrm{D}}}{A_{\mathrm{D}}+A_{\mathrm{E}}P} \quad (1)$$

$$\mathrm{IPCE_{S(D)}} = \mathrm{LHE_{S(D)}}\phi_{\mathrm{inj}}\eta_{\mathrm{C}} = \mathrm{LHE_{S(D)}APCE_{S(D)}} \quad (2)$$

where T_{FTO} is the transmittance of a conducting glass containing the effect of light reflection loss at an air/substrate glass interface, A_{D} the absorbance of a dye adsorbed TiO_2 film, A_{E} the absorbance of the electrolyte with the same thickness as the TiO_2 electrode, P the porosity of the TiO_2 electrode, ϕ_{inj} the quantum yield of charge injection, η_{C} the efficiency of collecting the injected charge at the conducting glass support, and APCE the absorption photon-to-current conversion efficiency.

The LHE and the IPCE of a tandem cell that consists of two DSCs with different dyes connected parallel is described as:

$$\mathrm{LHE}_{T(\mathrm{D1,D2})} = \mathrm{LHE_{S(D1)}} + T_{\mathrm{FTO}}T_{\mathrm{Pt}}10^{-(A_{\mathrm{D1}}+A_{\mathrm{E}}P+A_{\mathrm{E}}L/w)}\mathrm{LHE_{S(D2)}} \quad (3)$$

$$\mathrm{IPCE}_{\mathrm{T(D1,D2)}} = \mathrm{IPCE_{S(D1)}} + T_{\mathrm{FTO}}T_{\mathrm{Pt}}10^{-(A_{\mathrm{D1}}+A_{\mathrm{E}}P+A_{\mathrm{E}}L/w)}\mathrm{IPCE_{S(D2)}} \quad (4)$$

where T_{Pt} is the transmittance of a platinum sputtered conducting glass (counter electrode, CE), w the thickness of the TiO_2 electrode, and L the thickness of the bulk electrolyte layer between the TiO_2 electrode and the counter electrode.

An absorption model for DSC with scattering layer was constructed with a simple assumption that the incident light is reflected at the scattering layer and the light path length is extended twice as long as the single cell without scattering layer. The LHE and the IPCE of a single cell with scattering layer is described as:

$$\mathrm{LHE_{SC(D)}} = \mathrm{LHE_{S(D)}}\left(1 + 10^{-(A_{\mathrm{D}}+A_{\mathrm{E}}P)}\right) \quad (5)$$

$$\mathrm{IPCE_{SC(D)}} = \mathrm{LHE_{SC(D)}APCE_{S(D)}} \quad (6)$$

In this report, the IPCE was calculated using the value of $\mathrm{APCE_{N719}} = 1$ and $\mathrm{APCE_{BD}} = 0.8$.

3. Experimental

3.1. Sample preparation

Transparent nanocrystalline TiO_2 films were prepared as follows. A TiO_2 paste (Nanoxide-T, Solaronix) was deposited on a conducting glass substrate (F-doped SnO_2, sheet resistance = 10 Ω/square Nippon Sheet Glass) by doctor-blade method, followed by sintering at 500 °C for 30 min in a furnace. A scattering TiO_2 paste was prepared using a paste containing large TiO_2 particles (HPW-300C, diameter = ca. 300 nm, CCI). Scattering layer was deposited on the transparent sintered TiO_2 layer by doctor-blade method, and the film was sintered again at 500 °C for 30 min. The prepared TiO_2 film was cut into a suitable size. The thickness of the films was measured by a surface profiler (DEKTAK3, Solan). The porosity of TiO_2 film was calculated using the density of the actual porous TiO_2 film and the density of the TiO_2 anatase crystal (3.9 g cm^{-3}). The films were heated to 500 °C for 30 min again and cooled to 150 °C. After the cooling, the films were immersed in a 3.0×10^{-4} M of *cis*-dithiocyanate-*N*,*N*′-bis-(4-carboxylate-4-tetrabutylammoniumcarboxylate-2,2′-bipyridine) ruthenium(II) (N719, Ruthenium TBA 535, Solaronix) acetonitrile/2-methyl-2-propanol = 1/1 (v/v) solution or 2.0×10^{-4} M of trithiocyanate-*N*,*N*′,*N*″-4,4′,4″-tricarboxylate-2,2′,6,2″-terpyridine ruthenium(II) (black dye, Solaronix) and 2.0×10^{-2} M of taurochenodeoxycholic acid sodium salt (Sigma) in ethanol for 18 h. The resulting electrode was rinsed with acetonitrile or ethanol. After drying at room temperature, the porous electrode was covered by a CE. All CEs used in this report were semitransparent (transmittance of Pt = ca. 0.8) Pt sputtered conducting glass with light black outlook therefore the light reflection effect of counter electrode should be negligible. The Effective area of the cell electrode was set to 0.25 cm^2. The gap between the conducting glass substrate and the CE was sealed by a thermal adhesive film (HIMILAN, thickness = 25 μm, Mitsui–Dupont Polychemical). An electrolyte was prepared dissolving 0.6 M 1,2-dimethyl-3-propylimidazolium iodide, 0.1 M lithium iodide, 0.05 M iodine, and 0.5 M 4-*tert*-butylpyridine to methoxyacetonitrile solvent. The electrolyte was injected from a hole made on the counter electrode, and then the hole was sealed by a cover glass (Iwaki Glass) and the HIMILAN film.

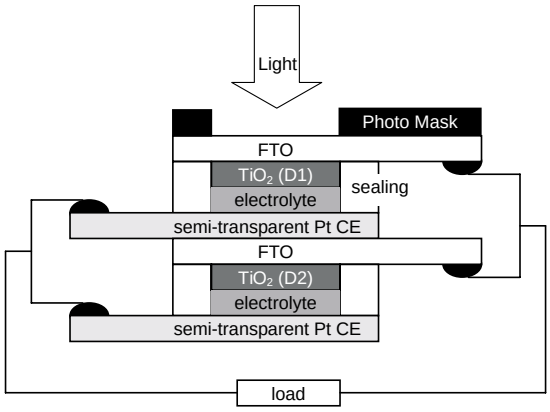

Fig. 1. The cross-sectional illustration of the tandem cell.

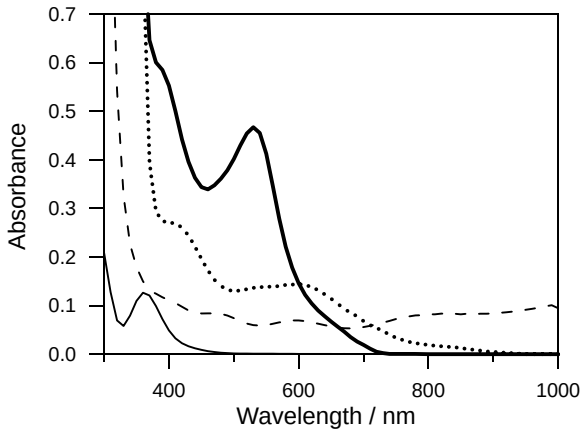

Fig. 2. Absorption spectra of the dye adsorbed TiO_2 films (N719, $w = 2.7\,\mu m$, bold solid curve; black dye $w = 2.5\,\mu m$, bold dotted curve), the electrolyte (thickness $= 10\,\mu m$, solid curve), and conducting glass (dashed curve) under comparable conditions.

3.2. Measurements

Absorption spectra were measured using transmission UV-Vis spectrometer (U-3300, Hitachi). When the absorption spectra of a conducting glass with TiO_2 film, a counter electrode, and a conducting glass were measured, a substrate was combined with a slide glass, and methoxyacetonitrile solvent was introduced into the space between the substrate and the slide glass to ignore the difference of refractive index between air and the solvent or the effect of solvatochromism of the dyes. The absorption spectra for dye adsorbed TiO_2 films were calculated using the absorption spectra of conducting glass with and without dye adsorbed TiO_2 film. A_E was calculated using the absorption spectrum of electrolyte as a function of TiO_2 thickness. Incident light was irradiated from substrate side in the measurement for the TiO_2 electrodes and the conducting glass or from the slide glass side in the measurement of the CE. The *I–V* characteristics of DSCs were evaluated using a solar simulator (YSS-50A, Yamashita Denso) as an AM 1.5 light source and a PC controlled voltage current source/meter (R6246, Advantest). For the tandem cell measurement, two cells were piled up carefully and connected in parallel (Fig. 1). We adapted Japanese Industrial Standard for amorphous solar cells in the cell efficiency determination [13]. IPCE measurements were carried out using a commercial setup for IPCE measurement (PV-25DYE, JASCO). The *I–V* characteristics and the IPCE measurements were carried out using a light mask with a $0.25\,cm^2$ window put on the top of cell (Fig. 1) to obtain accurate values.

4. Results and discussion

4.1. Evaluation of the absorption model

The IPCE spectrum of a single N719 cell was measured and calculated to evaluate the absorption model. To calculate the IPCE spectrum, the absorption spectra of the dye-adsorbed TiO_2 electrodes, the electrolyte, and the conducting glass were measured (Fig. 2). The absorption spectra were measured using transmission absorption spectrometer with the reference of the air, hence the effect of light reflection loss at an air/substrate glass interface were included in the spectrum for the conducting glass. Since the absorption coefficient of MLCT for black dye is about a half of that for N719 and the amount of dye adsorption on TiO_2 electrode for black dye is smaller than that for N719 [3,10], the absorbance of black dye adsorbed TiO_2 electrode was lower than that of N719 below 600 nm wavelength region. However, in the longer wavelength region (> 600 nm), black dye adsorbed TiO_2 electrode exhibited higher absorbance than N719 electrode. The electrolyte exhibited a peak of absorption at 360 nm corresponding to the absorption of I_3^- [14].

A measured IPCE spectrum and a calculated IPCE spectrum using Eqs. (1) and (2) were shown in Fig. 3. The calculated IPCE spectrum exhibited excellent agreement with the

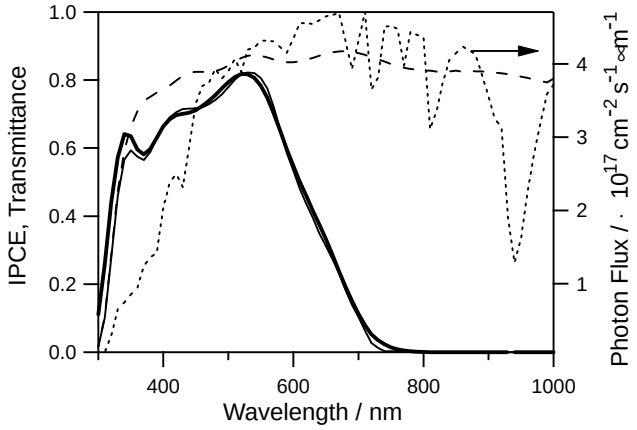

Fig. 3. Measured (bold solid curve) and calculated (solid curve) IPCE spectra for single DSC ($w = 7.7\,\mu m$) using N719 dye, the transmittance of conducting glass (dashed curve) and AM 1.5 photon flux (right axis, dotted curve).

measured one when APCE was set to unity, confirming the literature [2,3]. A deviation found in the shorter wavelength region (< 350 nm) would be caused in the measurement of the conducting glass absorption since the transmittance of the conducting glass showed identical values to the measured IPCE in the wavelength region. The absorption of the conducting glass was measured without TiO_2 film to avoid the difficulties to separate the absorption of the TiO_2 film, and then the difference of the refractive index should appear in the wavelength in which conducting glass has strong absorption.

Short-circuit photocurrent density (J_{SC}) was described as [15]:

$$J_{SC} = \int qF(\lambda)\mathrm{IPCE}(\lambda)\,\mathrm{d}\lambda \quad (7)$$

where q is the electron charge and $F(\lambda)$ the incident photon flux of the solar light. In this report, the effect of incident light loss at an air/substrate glass interface was included in IPCE. The calculated J_{SC} using calculated IPCE with Eq. (7) and AM 1.5 photon flux [6] described in Fig. 3 (right axis) showed excellent agreement with that obtained using measured IPCE (J_{SC} (cal) = 11.8 mA cm^{-2}, J_{SC} (mes) = 12.1 mA cm^{-2}), supporting the adequacy of the assumption in the model.

4.2. Possibility of photocurrent improvement by the introduction of the tandem structure

TiO_2 thickness dependent IPCE for N719 and black dye cell was investigated to estimate the possibility of photocurrent improvement by the tandem structure. The results were described in Fig. 4. The IPCE for N719 cell with 4.9 and 11.4 μm thickness exhibited relatively high value at shorter wavelength. Considering the light reflection and absorption of the conducting glass, almost all photons absorbed by the dyes were converted to photocurrent. IPCE for N719 cell

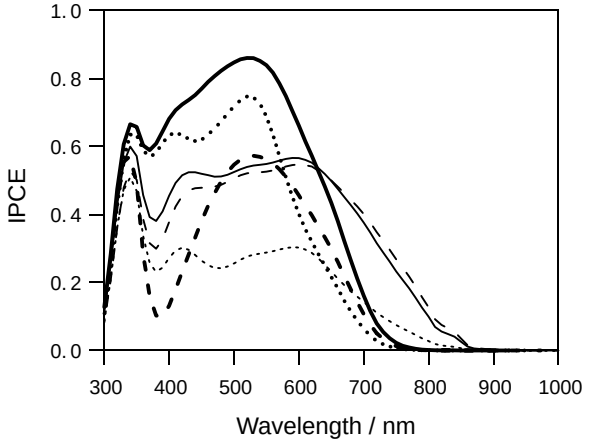

Fig. 4. The IPCE spectra for N719 and black dye cells with different TiO_2 thickness (N719, w = 4.9 μm bold dotted curve, w = 11.4 μm bold solid curve, and w = 19.6 μm bold dashed curve; black dye, w = 4.8 μm dotted curve, 12.0 μm solid curve, and 19.6 μm dashed curve).

with 4.9 μm TiO_2 film exhibited low values in longer wavelength region (600 < λ < 800 nm) because of its poor light absorption. This poor absorption in the longer wavelength region was partially improved by using thicker TiO_2 film. The IPCE for N719 DSC with 11.4 μm TiO_2 film exhibited higher value than that with 4.9 μm especially in the longer wavelength region. However, using thicker TiO_2 film does not lead to the extension of spectral response to the wavelength longer than 800 nm. The maximum IPCE values for black dye cells were less than 0.6. Considering the absorbance of the black dye adsorbed TiO_2 films, their APCE were 0.6–0.8. However, black dye cell exhibited higher IPCE value than N719 cell at higher wavelength region. Especially, black dye cell exhibited photocurrent in the longer wavelength region (> 800 nm) in which N719 cell has no spectral response. Hence, the incident light passing through the N719 cell can be absorbed by black dye cell, and then total photocurrent can be increased. These results support that the possibility of photocurrent improvement by the introduction of the tandem structure.

In our results, the decrease of IPCE with further increase of the thickness (> 12 μm) was observed for N719 cell and not observed for black dye cell. The reason of this photocurrent decrease with the increasing of film thickness in N719 cell was investigated. The amount of adsorbed N719 dye increased with the thickness of the TiO_2 electrode and saturated around 12 μm (adsorbed N719 amount for the film thickness 4.5, 6.8, 12, and 16 μm were 0.35, 0.66, 1.1, and 1.1 × 10^{-7} mol cm^{-2}, respectively). The amount could not be increased by the increasing of the dye concentration or increase of the dipping time in the dye solution. The inhomogeneous distribution of adsorbed dye across the film thickness for N719 could be caused by its larger molecular size (N719 has 1.7 times larger molecular weight than that of black dye). The poor coverage of dye on TiO_2 should increase in the probability of the charge recombination from TiO_2 electrode to I_3^- in the electrolyte. Not only the decrease of J_{SC}, but also the larger decrease of V_{OC} with increasing of film thickness for N719 cell (V_{OC} for N719 cell with film thickness 4.9, 11.4, 19.6 μm were 0.74, 0.71, and 0.67 V, respectively) than for black dye cell (V_{OC} for black dye cell with film thickness 4.8, 12, 19.6 μm were 0.66, 0.64, and 0.63 V, respectively) could support this explanation.

4.3. Solar cell performance of the tandem cell

A tandem cell was fabricated using N719 cell as a top cell and black dye cell as a bottom cell, and two cells were connected in parallel (Fig. 1). The measured and calculated IPCE spectra of the tandem cell are shown in Fig. 5. These IPCE spectra exhibited an excellent agreement, supporting that the assumption in the model is adequate. The tandem cell exhibited high IPCE values in the shorter wavelength region corresponding to N719 cell, and an extended spectral response in the longer wavelength region originated from the black dye cell. As a result, the tandem cell exhibited

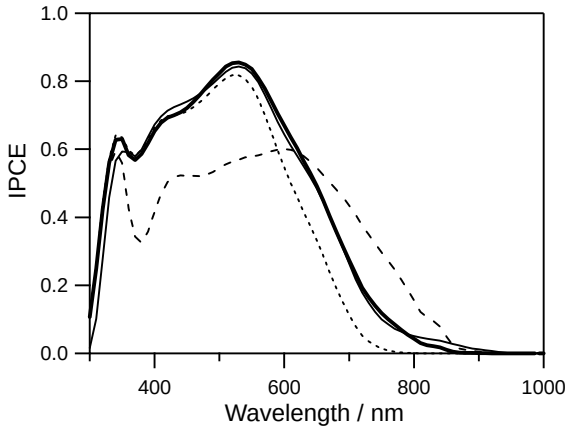

Fig. 5. Measured (bold solid curve) and calculated (solid curve) IPCE spectrum for the tandem DSC using N719 and black dye ($w_{N719} = 7.7\,\mu m$, $w_{BD} = 9.9\,\mu m$) and measured IPCE spectra for single N719 ($w = 7.7\,\mu m$, dotted curve) and black dye ($w = 9.9\,\mu m$, dashed curve) cell.

extended spectral response in longer wavelength range in which N719 cells have no response without loosing IPCE at shorter wavelength region. The *I–V* characteristics of the cells were shown in Fig. 6 and Table 1. The tandem cell exhibited about 20% higher photocurrent than N719 or black dye cell since its high IPCE in the shorter wavelength region and the extended spectral response in the longer wavelength region. The extended spectral response in the longer wavelength region should contribute to the increase of the photocurrent significantly because the solar light has large photon flux in 500–1000 nm. In general, single DSCs using black dye tend to exhibit lower open circuit photovoltage (V_{OC}) than that using N719 [10,11]. Here, the black dye cell exhibited lower V_{OC} than the N719 cell by 0.05 V. The tandem cell exhibited a similar value of V_{OC} to the black

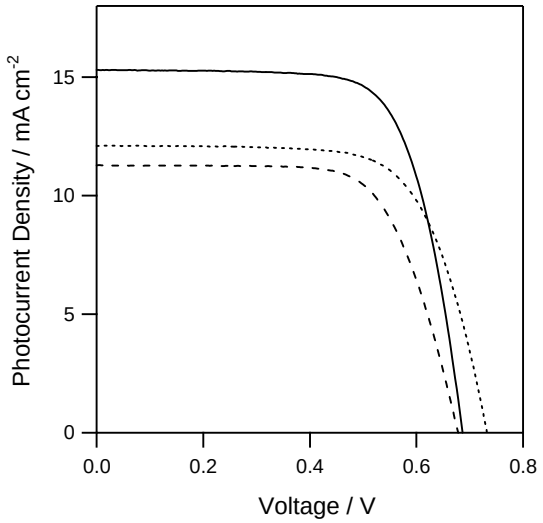

Fig. 6. *I–V* characteristics for the tandem DSC ($w_{N719} = 7.7\,\mu m$, $w_{BD} = 9.9\,\mu m$, solid curve) and the single DSCs (N719, $w = 7.7\,\mu m$, dotted curve; black dye $= 9.9\,\mu m$, dashed curve) measured under AM 1.5, 100 mW cm^{-2} irradiation.

Table 1
I–V characteristics of tandem DSCs and single DSCs

Sample	w (μm)	J_{SC} (mA cm^{-2})	V_{OC} (V)	FF	η (%)
N719	7.7	12.1	0.73	0.69	6.1
N719 (S)[a]	10.2	13.9	0.74	0.65	6.7
Black dye	9.9	11.3	0.68	0.66	5.2
Black dye (S)[a]	12.6	13.6	0.68	0.66	6.1
Tandem (N + BD)	7.7 + 9.9	15.3	0.67	0.71	7.3
Tandem (N + BD (S))[a]	7.7 + 12.6	15.9	0.69	0.70	7.6

All samples were measured under AM 1.5, 100 mW cm^{-2}. The cell areas were 0.25 cm^{-2}.

[a] With scattering layer (the thickness of small TiO_2 particle (first layer) in the TiO_2 film with scattering layer (first plus second layer) was same as corresponding TiO_2 film without scattering layer).

dye cell, however, the enhancement of photocurrent competed with the decrease of V_{OC}, and then the improvement of conversion efficiency was observed in the tandem cell.

4.4. Effect of scattering layer

Some large metal oxide particles were used as a scattering layer of DSC to enhance the light path length that allows increasing LHE at the longer wavelength region ($600 < \lambda < 800$ nm) in a N719 DSC [7]. Here, N719 DSC with scattering layer was fabricated to evaluate the effect of photocurrent increase and to make a comparison with the tandem cell. Measured and calculated IPCE spectra for N719 DSC with scattering layer were shown in Fig. 7. DSC with scattering layer exhibited an improved IPCE value at the longer wavelength region because of its extended light path length. The measured IPCE spectrum for the cell with scattering layer at longer wavelength region (> 600 nm) was well reproduced by calculated one with the simple assumption of twice of light path length, but exhibited lower value in the region of 400–600 nm. Since the scattering probability could depend on the ratio of wavelength and the size of the scattering particle, the effective light path length of the cell with

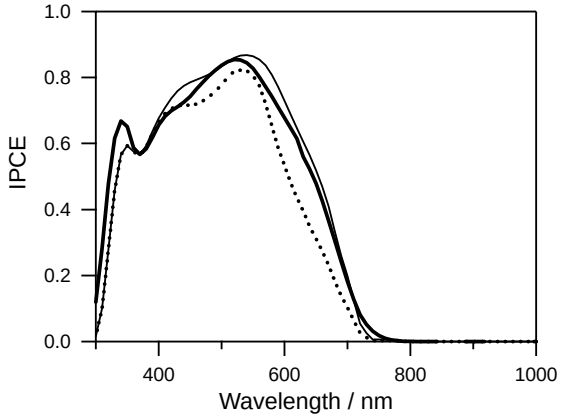

Fig. 7. Measured (bold solid curve) and calculated (solid curve) IPCE spectra for N719 DSC with scattering layer (=10.2 μm) and measured IPCE spectrum for N719 DSC without scattering layer ($w = 7.7\,\mu m$, bold dotted curve).

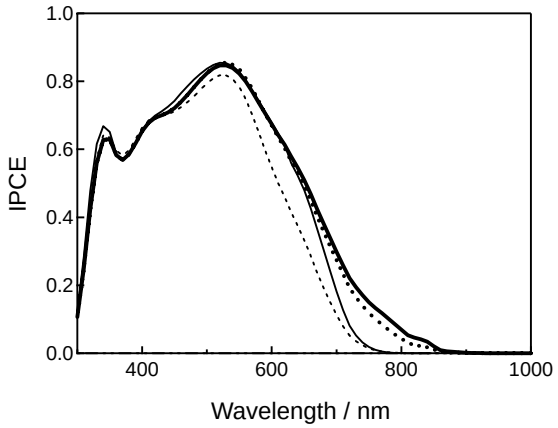

Fig. 8. Measured IPCE spectra for the tandem DSCs using N719 and black dye (with scattering layer on the second cell, w_{N719} = 7.7 μm, w_{BD} = 12.6 μm, bold solid curve; without scattering layer, w_{N719} = 7.7 μm, w_{BD} = 9.9 μm, bold dotted curve) and the single DSCs using N719 (with scattering layer, w = 10.2 μm, solid curve; without scattering layer, w = 7.7 μm, dotted curve).

scattering layer was probably shorter than twice of that of the cell without scattering layer in this region. The *I–V* characteristics of the single cell with scattering layer were described in Table 1. The introduction of the scattering layer improved photocurrent without decreasing photovoltage, but a little decreased FF that may be caused by increasing of photocurrent density. As a result the introduction of the scattering layer improved the efficiency of DSC.

The IPCE spectra of the tandem DSC and the single DSC with and without the scattering layer were shown in Fig. 8. The tandem cell and the single cell with the scattering layer showed similar IPCE spectra up to 650 nm, however, the tandem cell exhibited higher IPCE value than the later cell in the longer wavelength region (> 650 nm) since its bottom cell, black dye cell, has large spectral response in that wavelength region. A tandem cell with scattering layer in the bottom cell showed a slight improvement of IPCE in the longer wavelength region (> 700 nm) compared to the tandem cell without scattering layer and succeeded to convert more photons to current. The *I–V* characteristics of these cells were summarized in Table 1. The tandem cell exhibited higher J_{SC}, slightly lower V_{OC}, and a little higher FF (should be explained by lower photocurrent densities for each cell) than the single N719 cell with the scattering layer. As a result, the tandem cell exhibited higher conversion efficiency than the single N719 cell with the scattering layer. Finally, the combination of tandem cell and scattering layer allowed obtaining the highest photocurrent and conversion efficiency.

5. Conclusions

Advantages of tandem structure as a method to improve the photocurrent of DSC was theoretically and experimentally proved. The absorption model of the single cell was introduced and examined using experimental result. The calculated IPCE showed excellent agreement with the measured one. The possibility of photocurrent improvement by tandem structure was explained by the IPCE measurements for the single N719 and black dye cells. The fabricated tandem cell exhibited the improved spectral response, higher photocurrent, and higher conversion efficiency than the single cells. In the comparison of the tandem cell to the single cell with scattering layer, the tandem cell exhibited higher photocurrent, slightly lower V_{OC}, a little higher FF, and higher conversion efficiency than the single cell with scattering layer. The tandem cell with scattering layer in the bottom cell exhibited the highest photocurrent and conversion efficiency.

Regarding to the production cost of tandem cell, DSC has flexibility in the structure and the production cost can be reduced by the optimization of the cell structure. For example, we already fabricated a tandem cell with only two conducting glass plates, such as FTO/dye1–TiO_2/semitransparent conducting film/dye2–TiO_2/FTO, and observed the extension of the spectral response and short circuit photocurrent, where two conducting glass plates, the most expensive component of this type of solar cell, were omitted compare to the present structure. Unfortunately this cell exhibited lower FF and efficiency than corresponding single cells at this moment. We believe there is a possibility in the cost effectiveness of the tandem cell by the optimization of the cell structure and materials.

The tandem structure in DSC was presented as a valuable method to improve photocurrent and conversion efficiency. The model described in this report is valuable to predict the optimized cell configuration to maximize photocurrent from the absorption spectra of the components.

Acknowledgements

This work was partially supported by Open Competition for the Development of Innovative Technology (No. 12310) in Grant-in-Aid for the Creation of Innovations through Business-Academic-Public Sector Co-operation from the Ministry of Education, Culture, Sports, Science and Technology of Japan and the Strategic Research Base, Frontier Research Centre (Graduate School of Engineering) Osaka University, supported by the Japanese Government's Special Co-ordination Fund for Promoting Science and Technology. We are grateful to Mr. Teruhisa Inoue, Nippon Kayaku Co. Ltd., for providing dye samples and Mr. Kunio Kondo, Showa Denko K.K. for helpful suggestion. W.K. acknowledges to the Research Fellowship of Japan Society for the Promotion of Science for Young Scientists.

References

[1] B. O'Regan, M. Grätzel, Nature 353 (1991) 737.
[2] Md.K. Nazeeruddin, A. Kay, I. Rodicio, R. Hamphry-Baker, E. Müeller, P. Liska, N. Vlachopoulos, M. Grätzel, J. Am. Chem. Soc. 115 (1993) 6382.

[3] Md.K. Nazeeruddin, S.M. Zakeeruddin, R. Humphry-Baker, M. Jirousek, P. Liska, N. Vlachopoulos, V. Shklover, C. Fischer, M. Grätzel, Inorg. Chem. 38 (1999) 6298.
[4] K. Sayama, H. Sugihara, H. Arakawa, Chem. Mater. 10 (1998) 3825.
[5] S. Burnside, J.-E. Moser, K. Brooks, M. Grätzel, J. Phys. Chem. B 103 (1999) 9328.
[6] Japanese Industrial Standard Committee, Japanese Industrial Standard, Secondary Reference Amorphous Solar Cells, vol. JIS C 8931, Japanese Standards Association, Tokyo, 1995.
[7] A. Kay, M. Grätzel, Solar Energy Mater. Solar Cells 44 (1996) 99.
[8] A. Usami, Chem. Phys. Lett. 277 (1997) 105.
[9] S. Nishimura, N. Abrams, B.A. Lewis, L.I. Halaoui, T.E. Mallouk, K.D. Benkstein, J. van de Lagemaat, A.J. Frank, J. Am. Chem. Soc. 125 (2003) 6306.
[10] Md.K. Nazeeruddin, P. Péchy, T. Renouard, S.M. Zakeeruddin, R. Humphry-Baker, P. Comte, P. Liska, L. Cevey, E. Costa, V. Shklover, L. Spiccia, G.B. Deacon, C.A. Bignozzi, M. Grätzel, J. Am. Chem. Soc. 123 (2001) 1613.
[11] A. Islam, H. Sugihara, M. Yanagida, K. Hara, G. Fujihashi, Y. Tachibana, R. Katoh, S. Murata, H. Arakawa, New J. Chem. 26 (2002) 966.
[12] M.A. Green, Prog. Photovolt. Res. Appl. 9 (2001) 123.
[13] Japanese Industrial Standard Committee, Japanese Industrial Standard, Solar Simulators for Amorphous Solar Cells and Modules, vol. JIS C 8933, Japanese Standards Association, Tokyo, 1995.
[14] A. Popov, R.F. Swemsem, J. Am. Chem. Soc. 77 (1955) 3724.
[15] Y. Tachibana, K. Hara, K. Sayama, H. Arakawa, Chem. Mater. 14 (2002) 2527.